International Journal of Applied Engineering Research
ISSN 0973-4562 Volume 10, Number 6 (2015) pp. 14905-14921

http://www.ripublication.com

MHD Mixed Convection CU-Water Nano Fluid Flow With Viscous Dissipation Effects In The Presence Of Suction And Injection

M.Chandrasekar[1] and M.S.Kasiviswanathan[2]

Department of Mathematics, Anna University, Chennai-600 025, India.
[1]Telephone Number: +91-9444929475 e-mail: mchandru@annauniv.edu
[2]Telephone Number: +91-9840808079 e-mail: mskasi@gmail.com

Abstract

The variational solution of steady magneto hydrodynamic mixed convection boundary layer flow of Cu-water nanofluid over a semi-infinite flat plate in the presence of viscous dissipation, Joule heating and suction/injection effects is analyzed. Gyarmati's variational principle into non-equilibrium thermodynamics is employed to solve the problem. The governing boundary layer equations are approximated by simple fourth degree polynomial function and the variational principle is formulated over the region of boundary layer. The Euler-Lagrange equations of the principle are obtained as simple coupled equations in terms of momentum and thermal boundary layer thicknesses. The velocity and temperature profiles, the coefficient of skin friction and heat transfer rates are determined for different values of the Prandtl number *Pr*, magnetic parameter ξ, buoyancy parameter *Ri*, suction/injection parameter *H*, viscous dissipation parameter *Ec* and heat generation/absorption parameter *Q*. For some specific values of the parameters, the present results are compared with the available solutions in the literature and the comparison shows excellent agreement.

AMS Subject Classification: 80M30, 76-02, 76D05, 76D10, 76W05, 76R05, 76R10, 80A20

Key words: Gyarmati's variational principle; MHD; nanofluid; mixed convection; viscous dissipation; suction/injection.

1. Introduction

The objective of this research work is to analyze the heat transfer enhancement in two dimensional magnetohydrodynamic mixed convection boundary layer flow of a

nanofluid in the presence of viscous dissipation and suction/injection effects using a genuine variational principle developed by Gyarmati.

In recent years, nanofluid which is a mixture of nano-sized particles suspended in a base fluid is used to enhance the rate of heat transfer due to its higher thermal conductivity compared to the base fluid. The potential benefits of nanofluid are theoretically investigated by Choi [1] together with the experimental results of Masuda et al. [2]. Further these observations are confirmed by the experimental investigations of Xuan and Li [3]. The explanation for abnormal convective heat transfer enhancement observed in nanofluids is given by Buongiorno [4].

The effect of buoyancy forces on flow and heat transfer is usually neglected in high velocity forced convection flow. But in certain circumstances the buoyancy forces considerably influence the velocity and temperature fields in forced convection flow also. In such cases combined forced and free convection exists, which is called as mixed convection flow.

Magnetohydrodynamics is the study of the motion of an electrically conducting fluid in the presence of a magnetic field which plays an important role in boundary layer control and it is done by inducing current in a moving electrically conducting fluid.

Mixed convection flow over a non-isothermal wedge was analytically investigated by Antony Raj [5]. The boundary layer solution for mixed convection flow over a vertical plate in the presence of suction (or) injection was studied by Watanabe [6]. Aydin and Kaya [7] treated the ohmic heating and viscous dissipation effects on MHD mixed convection flow of a conventional fluid past a permeable vertical flat plate. Rana and Bhargava [8] numerically investigated the steady mixed convection nanofluid flow over a vertical flat plate with the effect of temperature dependent heat source/sink.

By considering all the above facts, in this study non-similar mixed convection flow of water based nanofluid containing the spherical shaped Copper (Cu) nanoparticles with volume fraction $\phi = 0.04$ over a semi-infinite flat plate in the presence of constant magnetic flux density, suction/injection, viscous dissipation and heat source/sink effects is analyzed. The Gyarmati's variational technique has been employed to solve the non-similar boundary layer equations. The computational results are given for velocity profile, temperature profile, the coefficient of skin friction (shear stress) and local Nusselt number (heat transfer) for various values of magnetic parameter ξ, buoyancy parameter Ri, viscous dissipation parameter Ec and suction/injection parameter H. The results obtained by the present analysis are compared with the results of regular fluid flow studied by Aydin and Kaya [7] and establishes the fact that the accuracy is remarkable. The main intention of this investigation is to justify that, the Gyarmati's variational technique is one of the most general and exact variational techniques in solving boundary layer flow and heat transfer problems. Chandrasekar [9, 10], Chandrasekar and Baskaran [11], Chandrasekar and Kasiviswanathan [12] already applied Gyarmati's variational technique for steady, unsteady heat transfer and boundary layer flow problems.

2. The governing equations and boundary conditions

The system of steady, two dimensional, incompressible and laminar boundary layer flow of nanofluid over a semi-infinite flat plate with suction and injection is considered. The leading edge of the plate is at $x = 0$, the plate is parallel to the x-axis and infinitely long downstream. In this study it is assumed that the flow is with free stream velocity U_∞ and the ambient temperature T_∞ which are parallel to x-axis and depending on its direction, the buoyancy forces may aid or oppose the main flow. And the temperature of the plate is held at a constant temperature T_0 which is greater than the ambient temperature T_∞. A uniform magnetic field of strength B_0 is applied normal to the x-axis and assumed that induced magnetic field is negligibly small. By employing Boussinesq-boundary layer approximations and with the assumption that all fluid properties are constants, the governing boundary layer equations for the present system are as follows

$$u_x + v_y = 0 \tag{1}$$

$$uu_x + vu_y = \frac{1}{\rho_{nf}}\left[\mu_{nf} u_{yy} + \kappa B_0^2 (U_\infty - u) + (\rho\beta)_{nf}\, g(T - T_\infty)\right] \tag{2}$$

$$uT_x + vT_y = \frac{1}{(\rho C_p)_{nf}}\left[k_{nf} T_{yy} + \mu_{nf} (u_y)^2 - \kappa B_0^2 u(U_\infty - u) + Q_0 (T - T_\infty)\right] \tag{3}$$

subject to the boundary conditions

$y = 0;\ u = 0,\ v = v_0,\ T = T_0,$

$y \to \infty;\ u = U_\infty =$ constant, $T = T_\infty$ (4)

Here u, v, v_0, T, κ, B_0, Q_0 and g are velocity of the fluid in x-direction, velocity of the fluid in y-direction, suction/injection velocity, temperature of the fluid, electric conductivity, externally imposed magnetic field in the y-direction, heat generation/absorption coefficient and acceleration due to gravity respectively.

The thermophysical properties of nanofluid namely density, dynamic viscosity, thermal diffusivity, volumetric expansion coefficient, heat capacity and thermal conductivity are denoted by ρ_{nf}, μ_{nf}, α_{nf}, $(\rho\beta)_{nf}$, $(\rho C_p)_{nf}$, k_{nf} respectively and have been calculated as functions of thermophysical properties of nanoparticle (spherical shaped) and base fluid as follows,

$$\begin{aligned}
\rho_{nf} &= (1-\phi)\rho_f + \phi\rho_s \\
\mu_{nf} &= \frac{\mu_f}{(1-\phi)^{2.5}} \\
\alpha_{nf} &= \frac{k_{nf}}{(\rho C_p)_{nf}} \\
(\rho\beta)_{nf} &= (1-\phi)(\rho\beta)_f + \phi(\rho\beta)_s \\
(\rho C_p)_{nf} &= (1-\phi)(\rho C_p)_f + \phi(\rho C_p)_s
\end{aligned} \tag{5}$$

and $$\frac{k_{nf}}{k_f} = \frac{k_s + 2k_f - 2\phi(k_f - k_s)}{k_s + 2k_f + \phi(k_f - k_s)}$$

Here ϕ is the particle volume fraction. The thermophysical properties of base fluid and nanoparticle are distinguished by subscripts f and s respectively.

3. Variational formulation of the problem

The purpose of this analysis is to obtain the approximate numerical solution of irreversible thermodynamics problem by a variational technique. Gyarmati [13, 14] developed a variational principle known as " Governing Principle of Dissipative Processes " (GPDP) which is given in its universal form

$$\delta \int_{V} (\sigma - \psi - \Phi)\, dV = 0. \tag{6}$$

The principle (6) describes the evaluation of linear, quasi linear and some nonlinear irreversible processes at any instant of time and space under constraints that the balance equations

$$\rho \dot{a}_i + \nabla \cdot \mathbf{J}_i = \sigma_i, \qquad (i = 1, 2, 3, \cdots f) \tag{7}$$

are satisfied. In Equation (6), δ is the variational symbol, σ is the entropy production, ψ and Φ are dissipation potentials and V is the total volume of the thermodynamic system. In Equation (7), ρ is the mass density and $\dot{a}_i$, $\mathbf{J_i}$, σ_i are respectively substantial variation, flux and source density of the i^{th} extensive transport quantity a_i. The entropy production σ per unit volume and unit time can always be written in the bilinear form

$$\sigma = \sum_{i=1}^{f} \mathbf{J}i \cdot \mathbf{X}i \geq 0 \tag{8}$$

where $\mathbf{J_i}$ and $\mathbf{X_i}$ are fluxes and forces respectively. According to Onsager's linear theory [15, 16] the fluxes are linear fuctions of forces, that is

$$\mathbf{J}_i = \sum_{k=1}^{f} L_{ik}\, \mathbf{X}_k, \qquad (i = 1, 2, 3, \cdots f) \tag{9}$$

or alternatively

$$\mathbf{X}_i = \sum_{k=1}^{f} R_{ik}\, \mathbf{J}_k, \qquad (i = 1, 2, 3, \cdots f) \tag{10}$$

The constants L_{ik} and R_{ik} are conductivities and resistances respectively satisfying the reciprocal relations [15, 16]

$$L_{ik} = L_{ki} \text{ and } R_{ik} = R_{ki}, \ (i, k = 1,2,3, \cdots f) \tag{11}$$

The matrices of L_{ik} and R_{ik} are mutually reciprocals and they are symmetric, that is

$$\sum_{m=1}^{f} L_{im} R_{mk} = \sum_{m=1}^{f} L_{mk} R_{im} = \delta_{ik}, \quad (i, k = 1, 2, 3, \cdots f) \tag{12}$$

where δ_{ik} is the Kronecker delta. The local dissipation potentials ψ and Φ are defined [15, 16] as,

$$\psi(\mathbf{X}, \mathbf{X}) = (1/2) \sum_{i,k=1}^{f} L_{ik} \mathbf{X}_i \cdot \mathbf{X}_k \geq 0 \tag{13}$$

$$\Phi(\mathbf{J}, \mathbf{J}) = (1/2) \sum_{i,k=1}^{f} R_{ik} \mathbf{J}_i \cdot \mathbf{J}_k \geq 0 \tag{14}$$

In the case of transport processes, the forces $\mathbf{X}_i$ can be generated as gradients of certain "Γ" variables and can be written as

$$\mathbf{X}_i = \nabla\Gamma_i \tag{15}$$

The principle (6) with the help of Equations (8), (13), (14) and (15), takes the form

$$\delta \int_{\mathrm{V}} \left[\sum_{i=1}^{f} \mathbf{J}_i \cdot \nabla\Gamma_i - (1/2) \sum_{i,k=1}^{f} L_{ik} \nabla\Gamma_i \cdot \nabla\Gamma_k - (1/2) \sum_{i,k=1}^{f} R_{ik} \mathbf{J}_i \cdot \mathbf{J}_k \right] d\mathrm{V} = 0 \tag{16}$$

This variational principle has been already applied for various dissipative systems and was established as the most general and exact variational principle of macroscopic continuum physics. For the description of viscous flow systems, Vincze [17] used the GPDP to derive the equations of thermodynamics. Many other variational principles have already been shown as partial forms of Gyarmati's principle.

The balance equations of the system play a central role in the formulation of Gyarmati's variational principle and hence the governing boundary layer Equations (1-3) are written in the balance form as

$$\nabla \cdot \mathbf{V} = 0, \qquad (\mathbf{V} = \mathbf{i}u + \mathbf{j}v) \tag{17}$$

$$\rho_{nf} (\mathbf{V} \cdot \nabla)\mathbf{V} + \nabla \cdot \overline{\overline{\mathrm{P}}} = (\kappa \mathrm{B}_0^2)\ U_\infty - (\mathbf{i} \cdot \mathbf{V})\ + (\rho\beta)_{nf}\, g(T - T_\infty)\mathbf{i} \tag{18}$$

$$(\rho C_p)_{nf} (\mathbf{V} \cdot \nabla)T + \nabla \cdot \mathbf{J}_q = \mu_{nf} (u_y^2) - (\kappa \mathrm{B}_0^2)(\mathbf{i} \cdot \mathbf{V})\ U_\infty - (\mathbf{i} \cdot \mathbf{V})\ + Q_0 (T - T_\infty) \tag{19}$$

These equations represent the mass, momentum and energy balances respectively. Here **i** and **j** being unit vectors in the directions of *x* and *y* axes respectively. In Equation (18) $\overline{\overline{\mathrm{P}}}$ denotes the pressure tensor which can be decomposed [13] as

$$\overline{\overline{\mathrm{P}}} = p\overline{\overline{\delta}} + \overset{\mathrm{o}}{\overline{\overline{\mathrm{P}}}}^{vs} \tag{20}$$

where *p* is the hydrostatic pressure, $\overline{\overline{\delta}}$ is the unit tensor and $\overset{\mathrm{o}}{\overline{\overline{\mathrm{P}}}}^{vs}$ is the symmetrical part of the viscous pressure tensor, whose trace is zero.

In the study of heat transfer and fluid flow problems, the energy picture of Gyarmati's principle is always advantageous over entropy picture. Therefore, the energy dissipation $T\sigma$ is used instead of entropy production σ. The energy dissipation for the present system is given [13] by,

$$T\sigma = -J_q (\partial lnT / \partial y) - P_{12} (\partial u / \partial y) \tag{21}$$

where J_q is the heat flux and P_{12} is the only component of momentum flux $\overset{\mathrm{o}}{\overline{\overline{\mathrm{P}}}}^{vs}$, satisfy the constitutive relations connecting the independent fluxes and forces as

$$J_q = -L_\lambda (\partial lnT / \partial y) \quad \text{and} \quad P_{12} = -L_s (\partial u / \partial y) \tag{22}$$

Here $L_\lambda = \lambda T$ and $L_\mathrm{s} = \mu$, where λ and μ are the thermal conductivity and viscosity respectively. With the help of Equations (22) the dissipation potentials in energy picture are found as follows

$$T\boldsymbol{\psi} = (1/2)\left[L_\lambda (\partial lnT / \partial y)^2 + L_s (\partial u / \partial y)^2 \right] \tag{23}$$

$$T\boldsymbol{\Phi} = (1/2)\left[R_\lambda J_q^2 + R_\mathrm{s} P_{12}^2 \right] \tag{24}$$

where $L_\lambda = R_\lambda^{-1}$ and $L_\mathrm{s} = R_\mathrm{s}^{-1}$.

Using Equations (21-24), Gyarmati's variational principle (6) is formulated in the

following form

$$\delta \int_0^l \int_0^\infty \left[\begin{array}{l} -J_q(\partial lnT/\partial y) - P_{12}(\partial u/\partial y) - (L_\lambda/2)(\partial lnT/\partial y)^2 \\ \qquad -(L_s/2)(\partial u/\partial y)^2 - (R_\lambda/2)J_q^2 - (R_s/2)P_{12}^2 \end{array} \right] dydx = 0, \qquad (25)$$

in which l is the representative length of the surface.

4. Method of solution

It is assumed that the trial functions for velocity and temperature fields inside the respective boundary layers are as follows

$$\begin{aligned} u/U_\infty &= 2y/d_1 - 2y^3/d_1^3 + y^4/d_1^4 \qquad (y < d_1) \\ u &= U_\infty \qquad (y \geq d_1) \\ (T - T_\infty)/(T_0 - T_\infty) &= \theta \\ &= 1 - 2y/d_2 + 2y^3/d_2^3 - y^4/d_2^4 \qquad (y < d_2) \\ T &= T_\infty \qquad (y \geq d_2) \end{aligned} \qquad (26)$$

where d_1, d_2 are the velocity and temperature boundary layer thicknesses which are to be determined from the variational procedure. The trial functions (26) satisfy the following compatibility conditions,

$y = 0$; $u = 0$, $v = v_0$, $T = T_0$, $\partial T/\partial y = 0$ (smooth fit), $\partial^2 T/\partial y^2 = 0$

$y = d_1$; $u = U_\infty$ = constant, $\partial u/\partial y = 0$

(smooth fit), $\partial^2 u/\partial y^2 = 0$ (27)

$y = d_2$; $T = T_\infty$, $\partial T/\partial y = 0$ (smooth fit)

The smooth fit conditions $\partial u/\partial y = 0$ and $\partial T/\partial y = 0$ correspond to $P_{12} = 0$ and $J_q = 0$ at their respective edges of the boundary layer. Using the boundary conditions (27), the transverse velocity component v is obtained from the mass balance equation (17) as

$$v = U_\infty (4y^5/5d_1^5 - 3y^4/2d_1^4 + y^2/d_1^2) d_1' + v_0, \qquad (28)$$

where v_0 is the suction/injection velocity.

The velocity and temperature functions (26) and the boundary conditions (27) are used in the governing boundary layer Equations (17-19) and on direct integration with respect to y with the help of their corresponding smooth fit conditions $u_y = 0$ and $T_y = 0$, the momentum flux P_{12} and energy flux J_q are obtained. The momentum flux P_{12} remains the same for any Prandtl number Pr but the energy flux J_q has different expressions for $Pr \leq 1$ and $Pr \geq 1$. When $Pr \leq 1$ the expression for J_q in the range $d_1 \leq y \leq d_2$ is obtained first and the expression for J_q in the range $0 \leq y \leq d_1$ is determined subsequently by matching the expressions of the two regions at the interface. The expressions for momentum and the energy fluxes P_{12} and J_q are obtained respectively as follows,

$$
\begin{aligned}
-P_{12}/L_s = {} & (U_\infty^2 d_1'/\upsilon_{nf})(-4y^9/45d_1^9 + 2y^8/5d_1^8 - 3y^7/7d_1^7 - 11y^6/15d_1^6 + 7y^5/5d_1^5 \\
& - 2y^3/3d_1^3 + 101/1800) + (v_0 U_\infty/\upsilon_{nf})(y^4/d_1^4 - 2y^3/d_1^3 + 2y/d_1 - 7/10) \\
& + (\kappa B_0^2 U_\infty/\mu_{nf})(y^5/5d_1^4 - y^4/2d_1^3 + y^2/d_1 - y + 7d_1/30) + U_\infty/d_1 \\
& - \beta_{nf} g(T_0 - T_\infty)/\upsilon_{nf}(-y^5/5d_2^4 + y^4/2d_2^3 - y^2/d_2 + y + d_1^5/30d_2^4 - d_1^4/10d_2^3 \\
& + d_1^2/3d_2 - d_1/2) \qquad (0 \le y \le d_1)
\end{aligned} \tag{29}
$$

$$
\begin{aligned}
-J_q/L_\lambda = {} & \left[U_\infty(T_0 - T_\infty)/\alpha_{nf}\right]\Big[d_2'(4y^9/9d_1^4 d_2^5 - y^8/d_1^3 d_2^5 - 3y^8/4d_1^4 d_2^4 + 12y^7/7d_1^3 d_2^4 \\
& + 4y^6/3d_1 d_2^5 + y^6/3d_1^4 d_2^2 - 12y^5/5d_1 d_2^4 - 4y^5/5d_1^3 d_2^2 + 4y^3/3d_1 d_2^2 + d_1^5/45d_2^5 \\
& - 9d_1^4/140d_2^4 + 2d_1^2/15d_2^2 - 3/10) + d_1'(-16y^9/45d_1^5 d_2^4 + 3y^8/5d_1^5 d_2^3 \\
& + 3y^8/4d_1^4 d_2^4 - 9y^7/7d_1^4 d_2^3 - 2y^6/3d_1^2 d_2^4 - 4y^6/15d_1^5 d_2 + 3y^5/5d_1^4 d_2 \\
& + 6y^5/5d_1^2 d_2^3 - 2y^3/3d_1^2 d_2 + 49d_1^4/180d_2^4 - 18d_1^3/35d_2^3 + d_1/3d_2) \\
& + (v_0/U_\infty)(-y^4/d_2^4 + 2y^3/d_2^3 - 2y/d_2 + d_1^4/d_2^4 - 2d_1^3/d_2^3 + 2d_1/d_2)\Big] \\
& + (U_\infty^2 \mu_{nf}/\alpha_{nf}(\rho C_p)_{nf})(-16y^7/7d_1^8 + 8y^6/d_1^7 - 36y^5/5d_1^6 - 4y^4/d_1^5 \\
& + 8y^3/d_1^4 - 4y/d_1^2 + 52/35d_1) + (\kappa B_0^2 U_\infty^2/\alpha_{nf}(\rho C_p)_{nf})(-y^9/9d_1^8 \\
& + y^8/2d_1^7 - 4y^7/7d_1^6 - 2y^6/3d_1^5 + 9y^5/5d_1^4 - y^4/2d_1^3 - 4y^3/3d_1^2 \\
& + y^2/d_1 - 37d_1/315) \qquad (0 \le y \le d_1); \quad (Pr \le 1)
\end{aligned} \tag{30}
$$

$$
\begin{aligned}
-J_q/L_\lambda = {} & \left[U_\infty(T_0 - T_\infty)d_2'/\alpha_{nf}\right](4y^5/5d_2^5 - 3y^4/2d_2^4 + y^2/d_2^2 - 3/10) \\
& (d_1 \le y \le d_2); \quad (Pr \le 1)
\end{aligned} \tag{31}
$$

$$
\begin{aligned}
-J_q/L_\lambda = {} & \left[U_\infty(T_0 - T_\infty)/\alpha_{nf}\right]\Big[d_2'(4y^9/9d_1^4 d_2^5 - y^8/d_1^3 d_2^5 - 3y^8/4d_1^4 d_2^4 + 12y^7/7d_1^3 d_2^4 \\
& + 4y^6/3d_1 d_2^5 + y^6/3d_1^4 d_2^2 - 12y^5/5d_1 d_2^4 - 4y^5/5d_1^3 d_2^2 + 4y^3/3d_1 d_2^2 \\
& - d_2^4/36d_1^4 + 3d_2^3/35d_1^3 - 4d_2/15d_1) + d_1'(-16y^9/45d_1^5 d_2^4 + 3y^8/5d_1^5 d_2^3 \\
& + 3y^8/4d_1^4 d_2^4 - 9y^7/7d_1^4 d_2^3 - 2y^6/3d_1^2 d_2^4 - 4y^6/15d_1^5 d_2 + 3y^5/5d_1^4 d_2 \\
& + 6y^5/5d_1^2 d_2^3 - 2y^3/3d_1^2 d_2 + d_2^5/45d_1^5 - 9d_2^4/140d_1^4 + 2d_2^2/15d_1^2) \\
& + (v_0/U_\infty)(-y^4/d_2^4 + 2y^3/d_2^3 - 2y/d_2 + 1)\Big] + (U_\infty^2 \mu_{nf}/\alpha_{nf}(\rho C_p)_{nf}) \\
& (16y^7/7d_1^8 - 8y^6/d_1^7 + 36y^5/5d_1^6 + 4y^4/d_1^5 - 8y^3/d_1^4 + 4y/d_1^2 \\
& - 16d_2^7/7d_1^8 + 8d_2^6/d_1^7 - 36d_2^5/5d_1^6 - 4d_2^4/d_1^5 + 8d_2^3/d_1^4 \\
& - 4d_2/d_1^2) + (\kappa B_0^2 U_\infty^2/\alpha_{nf}(\rho C_p)_{nf})(-y^9/9d_1^8 + y^8/2d_1^7 - 4y^7/7d_1^6 \\
& - 2y^6/3d_1^5 + 9y^5/5d_1^4 - y^4/2d_1^3 - 4y^3/3d_1^2 + y^2/d_1 + d_2^9/9d_1^8 \\
& - d_2^8/2d_1^7 + 4d_2^7/7d_1^6 + 2d_2^6/3d_1^5 - 9d_2^5/5d_1^4 + d_2^4/2d_1^3 + 4d_2^3/3d_1^2 \\
& - d_2^2/d_1) + (Q_0(T_0 - T_\infty)/\alpha_{nf}(\rho C_p)_{nf})(y^5/5d_2^4 - y^4/2d_2^3 + y^2/d_2 \\
& - y + 3d_2/10)) \qquad (0 \le y \le d_2); \quad (Pr \ge 1)
\end{aligned} \tag{32}
$$

The prime indicates differentiation with respect to *x*. Using the expressions of P_{12} and J_q together with velocity and temperature functions (26), the variational principle (25) is formulated independently for $Pr \leq 1$ and $Pr \geq 1$ cases. After performing the integration with respect to *y*, one can obtain the variational principle in the following forms,

$$\delta \int_0^l L_1[d_1, d_2, d_1', d_2']dx = 0, \ (Pr \leq 1) \tag{33}$$

$$\delta \int_0^l L_2[d_1, d_2, d_1', d_2']dx = 0, (Pr \geq 1) \tag{34}$$

where L_1, L_2 are the Lagrangian densities of the principle. The variation is carried out with respect to the independent parameters d_1 and d_2. These variational principles (33), (34) are found identical when $d_1=d_2$.

The Euler-Lagrange equations corresponding to these variational parameters are

$$(\partial L_{1,2}/\partial d_1) - (d/dx)(\partial L_{1,2}/\partial d_1') = 0 \tag{35}$$

$$(\partial L_{1,2}/\partial d_2) - (d/dx)(\partial L_{1,2}/\partial d_2') = 0, \quad (Pr \leq 1, Pr \geq 1) \tag{36}$$

where $L_{1,2}$ represents the Lagrangian densities L_1 and L_2 respectively. These Equations (35) and (36) are second order ordinary differential equations in terms of d_1 and d_2. The procedure for solving Equations (35) and (36) can be considerably simplified by introducing the non-dimensional boundary layer thicknesses d_1^* and d_2^* and are given by

$$d_1 = d_1^* \sqrt{\upsilon_f x / U_\infty} \qquad \text{and} \qquad d_2 = d_2^* \sqrt{\upsilon_f x / U_\infty} \tag{37}$$

These variational principles (33) and (34) are subject to the transformations (37). The resulting Euler-Lagrange equations are obtained as simple polynomial equations,

$$\partial L_{1,2}/\partial d_1^* = 0 \tag{38}$$

$$\partial L_{1,2}/\partial d_2^* = 0, (Pr \leq 1, Pr \geq 1) \tag{39}$$

The coefficients of these Equations (38) and (39) dependent on the independent parameters *Pr*, ξ, *Ri*, *H*, *Ec* and *Q*, where $Pr = \upsilon_f / \alpha_f$ (Prandtl number), $\xi = \kappa B_0^2 x / \rho U_\infty$ (magnetic parameter), $Ri=Gr/Re^2$ (Richardson number), $Gr = g\beta_f \ T_0 - T_\infty \ x^3 / \upsilon_f^2$ (Grashof number), $Re = U_\infty x / \upsilon_f$ (Reynolds number), $H = v_0 \sqrt{x / \upsilon_f U_\infty}$ (suction/injection parameter), $Ec = U_\infty^2 / C_p (T_0 - T_\infty)$ (Eckert number) and $Q = Q_0 x / U_\infty \ \rho C_p \ _f$ (heat generation / absorption parameter).

In the present analysis, the surface is heated, that is $T_0 - T_\infty > 0$. Hence, if free stream is in the direction of flow field then $Ri > 0$ (aiding buoyancy) and the buoyancy force accelerates the boundary layer flow. On the other hand if free stream is in the direction opposite to flow flied then $Ri < 0$ (opposing buoyancy) and the buoyancy force decelerates the boundary layer flow. The suction and injection are represented by $H < 0$ and $H > 0$ respectively. Equations (38) and (39) are simple coupled polynomial equations and it can be solved for any values of *Pr*, ξ, *Ri*, *H*, *Ec*,

Q and it is found that the obtained simultaneous solutions d_1^* and d_2^* are as the only one set of positive real roots. After obtaining the values of d_1^* and d_2^* for given Pr, ξ, Ri, H, Ec and Q, the values of velocity, temperature profiles, skin friction (shear stress) and heat transfer (Nusselt number) are calculated with the help of the following expressions,

$$\eta = y\sqrt{U_\infty/\upsilon_f x} \tag{40}$$

$$\tau_w = \sqrt{\upsilon_f x/U_\infty^3}\ (-P_{12}/L_s)_{y=0} \tag{41}$$

$$\text{and } Nu_l = \sqrt{\upsilon_f x/U_\infty (T_0 - T_\infty)^2}\ (J_q/L_\lambda)_{y=0}. \tag{42}$$

5. Analysis of Results

The main and important characteristics of the problem analyzed are skin friction and heat transfer values. The energy equation has been solved for two cases $d_1^* \le d_2^*\ (Pr \le 1)$ and $d_1^* \ge d_2^*\ (Pr \ge 1)$. These two independent analyses yield solutions and it is matching at $Pr = 1$. It is found that both the analyses lead to satisfactory results in the respective ranges of Pr.

The thermophysical properties of water for Pr = 6.2 and Cu-nanoparticle are given in Table 1 are used to compute Cu/water nanofluid.

Table 1: Thermophysical properties of water and copper nanoparticle.

	$\rho\ (kgm^{-3})$	$C_p\ (Jkg^{-1}K^{-1})$	$K\ (Wm^{-1}K^{-1})$	$\beta \times 10^{-5}\ (K^{-1})$
H_2O	997.1	4179	0.613	21
Cu	8933	385	401	1.67

It is customary that when a new mathematical method is applied to a problem, the obtained results are compared with the available solution in order to establish the accuracy of the results involved in the present technique.

In Table 2, the heat transfer values of regular fluid for various values of Pr ($Pr \le 1$ and $Pr \ge 1$) when $\xi = Ri = H = Ec = Q = 0$ are obtained by the present variational technique. From this table it is evidently clear that the present results are in good agreement with Lin and Lin [18], Yih [19] and Aydin and Kaya [7]. It is also observed that the heat transfer increases with the values of Prandtl number. Since the higher Prandtl number has very low thermal conductivity, the local Nusselt number increases rapidly. This means that the variation of the heat transfer rate is more sensitive to the larger Prandtl number than the smaller one.

Table 2: Local Nusselt number for various values of *Pr* when ξ = *Ri* = *H* = *Ec* = *Q* = ϕ =0.

Pr	Present Results Nu_l	Lin & Lin [18] Nu_l	Yih [19] Nu_l	Aydin & Kaya [7] Nu_l
0.01	0.054742313	0.051590	0.051589	0.051437
0.1	0.147754551	0.140032	0.140034	0.148123
1	0.334277544	0.332058	0.332057	0.332000
10	0.738452128	0.728148	0.728141	0.727801
100	1.599967934	1.57186	1.571831	1.573141

Table 3 displays the heat transfer values of regular fluid for various values of ξ, *Ec* with *Pr* = 0.733 and *Pr* = 1 when *Ri* = *H* = *Q* = *0*. From this table, the obtained heat transfer values from the present thermodynamic analysis are compared with Watanabe and Pop [20] and Aydin and Kaya [7]. The comparison is good with a high order of accuracy. From this table it is noted that heat transfer values are increasing with the magnetic parameter ξ and decreasing with *Ec*.

Table 3: Local Nusselt number as a function of ξ for various values of *Pr* and *Ec* when *Ri* = *H* = *Q* = ϕ = *0*.

Pr	ξ	Present Results		Watanabe & Pop [20]		Aydin & Kaya [7]	
		Ec=0.0	*Ec*=1.0	*Ec*=0.0	*Ec*=1.0	*Ec*=0.0	*Ec*=1.0
0.733	0.0	0.2997214322	0.1594322283	0.29755	0.12395	0.29753	0.17031
	0.5	0.3509466982	0.1917651052	0.35699	0.20871	0.35709	0.21012
	1.0	0.3786430015	0.2113702944	0.38336	0.28857	0.38363	0.22873
	1.5	0.3961867294	0.2381053043	0.39959	0.24122	0.40012	0.24082
	2.0	0.4084325641	0.2499078214	0.41091	0.25022	0.41134	0.24963
1.0	0.0	0.332775444	0.1590535671	0.33206	0.16603	0.33206	0.16599
	0.5	0.3911204994	0.1972096839	0.40280	0.20144	0.40259	0.20132
	1.0	0.4232045708	0.2105439783	0.43446	0.21727	0.43460	0.21710
	1.5	0.4444082310	0.2264237472	0.45413	0.22710	0.45302	0.22672
	2.0	0.4596797063	0.2296600733	0.46798	0.23401	0.46612	0.23296

In Table 4 the heat transfer values of regular fluid are compared with different values of *Ri* for the given values of *Pr* = 0.72 and *Pr* = 7.0 when ξ = *H* = *Ec* = *Q* = *0*. From this table it is evidently clear that the present results are in excellent agreement with Saeid [21] and Aydin and Kaya [7]. And it is clear that increasing buoyancy parameter *Ri* enhance the heat transfer rate since the buoyancy force assists the forced convection.

Table 4: Local Nusselt number for various values of *Pr* and *Ri* when $\xi = H = Ec = Q = \phi = 0$.

Ri	*Pr* = 0.72			*Pr* = 7.0		
	Present Results	Saeid [21]	Aydin & Kaya [7]	Present Results	Saeid [21]	Aydin & Kaya [7]
0.0	0.2978547930	0.309	0.297	0.6544374703	0.628	0.646
0.2	0.3335825118	0.332	0.332	0.6982300955	0.698	0.698
0.4	0.3624611405	0.361	0.356	0.7280952848	0.752	0.740
0.6	0.3829019386	0.382	0.376	0.7559220566	0.791	0.772
0.8	0.3976871037	0.402	0.392	0.7887513894	0.822	0.802
1.0	0.4087531592	0.416	0.406	0.8257116380	0.851	0.827

Based on the direction of external forced flow, the two different cases of aiding and opposing mixed convection are analyzed. In case of aiding mixed convection, external forced flow is considered in the same direction of buoyancy force caused by heated wall ($T_0 > T_\infty$) and so $Ri > 0$. This phenomenon is analyzed in figures 1-6. In the second case, the direction of external flow is assumed in the direction opposite to the buoyancy driven flow caused by heated wall therefore $Ri < 0$ and this case is called opposing mixed convection which decelerates the main flow due to adverse pressure gradient. This situation is discussed in the figures 7-12. And it is well known that the Grashof number (*Gr*) and Reynolds number (*Re*) are the influencing parameters of free and forced convection flows respectively. Hence the ratio, $Gr/Re^2 = Ri$ (Richardson number) is the controlling parameter in mixed convection flows. For small values of *Ri*, forced convection dominates the flow whereas free convection is the dominant mode when *Ri* takes the large values. All the figures are obtained for *Pr* = 6.2, corresponding to Cu-water nanofluid.

From figures 1 and 2, it can be easily observed that as buoyancy force increases accordingly, the non-dimensional velocity also increases and the temperature profile decreases. The velocity increase and temperature decrease are rapid in free convection dominated regime. In addition, magnetic parameter increases the velocity and decreases the temperature. The effect of ξ is more considerable in forced convection predominant regime when compared to free convection dominant regime.

Figures 3 and 4 represent the effects of suction / injection parameter *H* and viscous dissipation parameter *Ec* on velocity and temperature profiles respectively. From these figures it is observed that suction decreases the velocity and temperature profiles while injection increases them when compared to impermeable plate. In addition, the effect of an increase in viscous dissipation parameter *Ec* is to increase the temperature profile shown in figure 4.

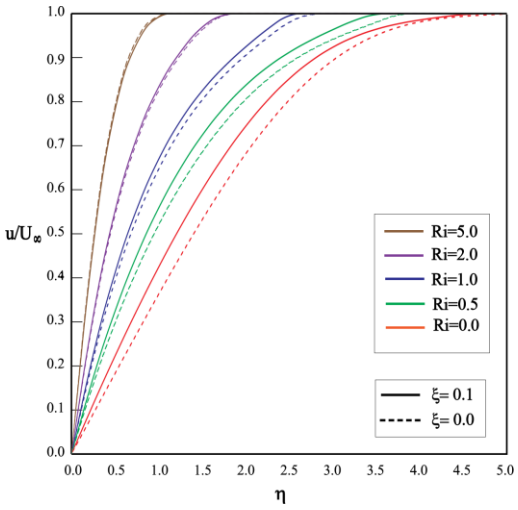

Figure 1: Velocity profile for different values of *Ri*(aiding-buoyancy) with *Pr* = 6.2 and ϕ = 0.04 when *H* = *Ec* = *Q* = *0*.

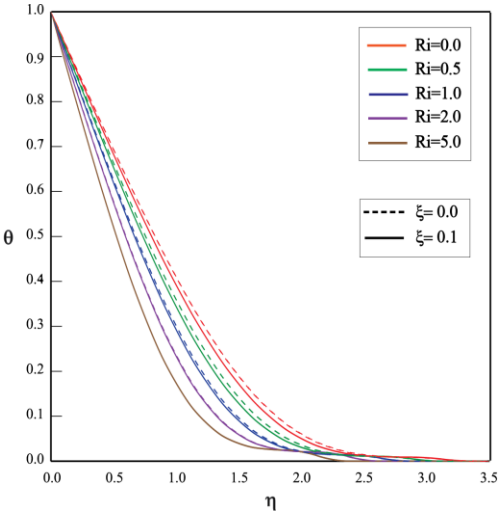

Figure 2: Temperature profile for different values of *Ri*(aiding-buoyancy) with *Pr* = 6.2 and ϕ = 0.04 when *H* = *Ec* = *Q* = *0*.

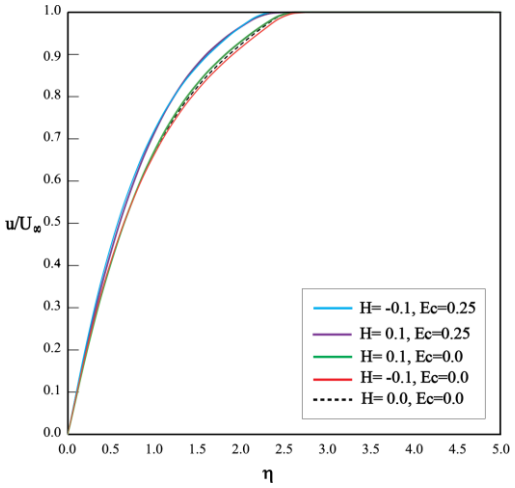

Figure 3: Velocity profile for different values of *H* and *Ec* with *Pr* = 6.2, ξ = 0.1, *Ri* = 1 and ϕ = 0.04 when *Q* = *0*.

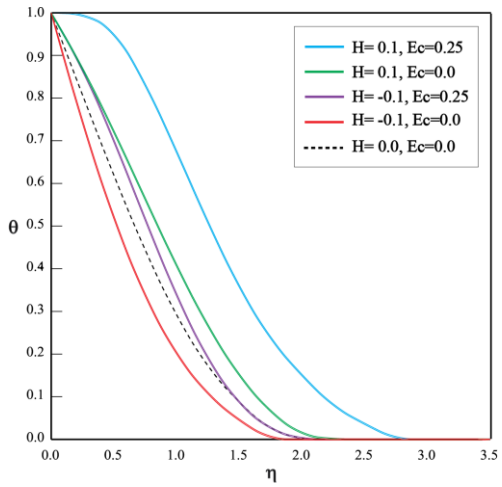

Figure 4: Temperature profile for different values of *H* and *Ec* with *Pr* = 6.2, ξ = 0.1, *Ri* = 1 and ϕ = 0.04 when *Q* = *0*.

Figures 5 and 6 describe the effects of skin friction and heat transfer values as a function of magnetic parameter ξ for different values of *Ri*, *H* and *Ec* respectively. From these figures it is observed that both skin friction and local Nusselt number (heat transfer) increases with buoyancy parameter *Ri* and magnetic parameter ξ irrespective of suction / injection parameter *H*. But the trend reverses in free convection predominant regime ($Ri \to \infty$), that is increasing magnetic parameter ξ decreases the local Nusselt number. And the skin friction increases as *Ec* increases. Contrarily local Nusselt number decreases with the increasing values of *Ec*. It is worth

mentioning to note that when the flow is controlled by injection, skin friction decreases as Eckert number *Ec* increases in free convection dominant regime (figure 5c). Also noted that the effect of *Ec* is significant in free convection dominant regime compared to forced convection dominant regime is shown in figures 5 and 6. As expected, suction increases the skin friction and local Nusselt number when compared to impermeable wall case, while the trend reverses in case of injection.

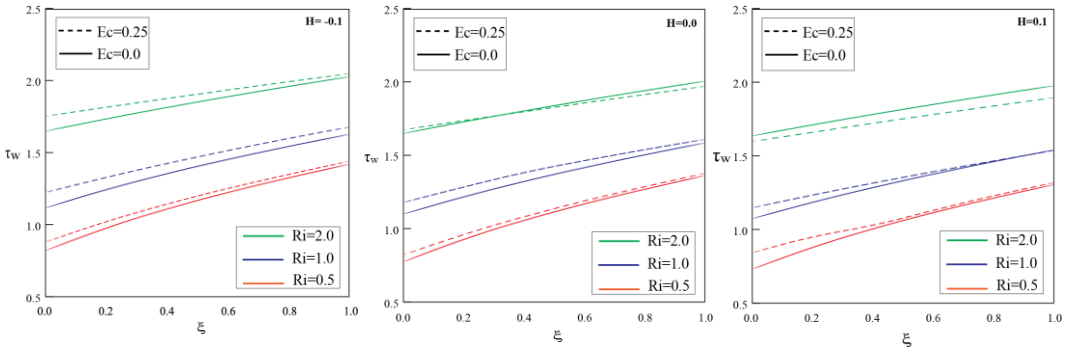

(*a*) (*b*) (*c*)

Figure 5: Effects of *Ri* (aiding-buoyancy), ξ and *Ec* on skin friction for (*a*) *H = -0.1* (suction), (*b*) *H = 0.0* and (*c*) *H = 0.1*(injection) with *Pr = 6.2* and *ϕ = 0.04* when *Q = 0.*

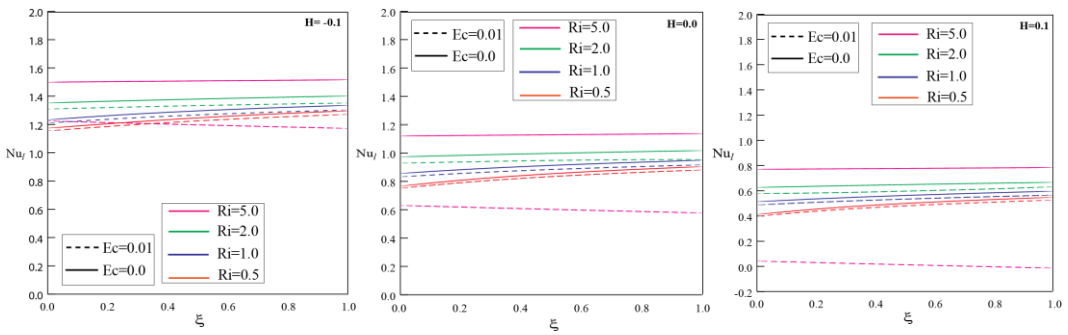

(*a*) (*b*) (*c*)

Figure 6: Effects of *Ri* (aiding-buoyancy), ξ and *Ec* on local Nusselt number for (*a*) *H = -0.1* (suction), (*b*) *H = 0.0* and (*c*) *H = 0.1*(injection) with *Pr = 6.2* and *ϕ = 0.04* when *Q = 0.*

For the case of opposing mixed convection flow, the velocity and temperature profiles for different values of the buoyancy parameter *Ri* are shown in figures 7 and 8. It is found that non dimensional velocity decreases as *Ri* increases due to the deceleration flow since the forced and free convection flows act in opposite directions. For increasing *Ri*, the temperature profile increases but the increase is not in significant level as shown in figure 8.

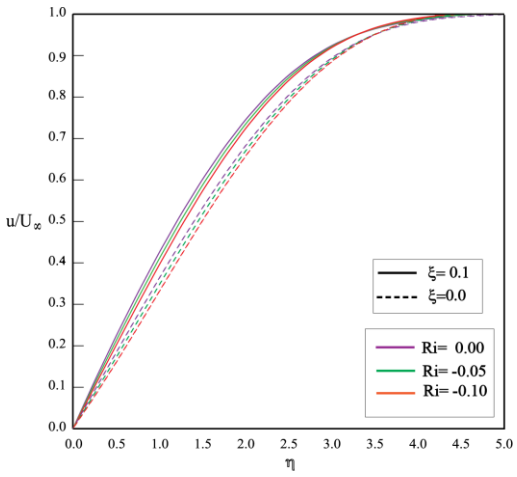

Figure 7: Velocity profile for different values of *Ri* (opposing-buoyancy) with *Pr* = 6.2 and ϕ = 0.04 when *H* = *Ec* = *Q* = *0*.

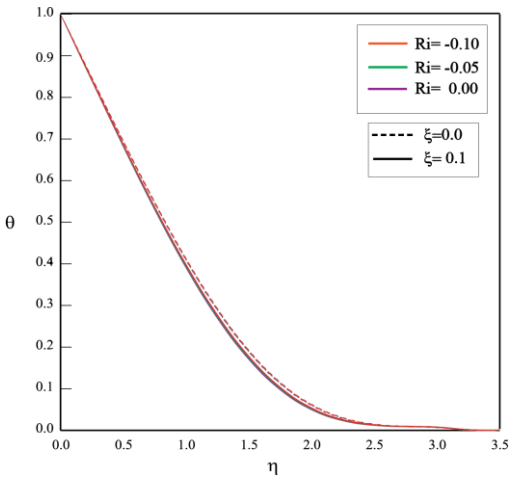

Figure 8: Temperature profile for different values of *Ri* (opposing-buoyancy) with *Pr* = 6.2 and ϕ = 0.04 when *H* =*Ec* = *Q* = *0*.

In figures 9 and 10, the effects of *H* and *Ec* on velocity and temperature profiles are illustrated. It is shown that the suction increases the velocity while injection decreases it when compared to impermeable flat plate and the trend is opposite in temperature profile shown in figure 10. Again the increasing values of viscous dissipation (*Ec*) increases the temperature profile.

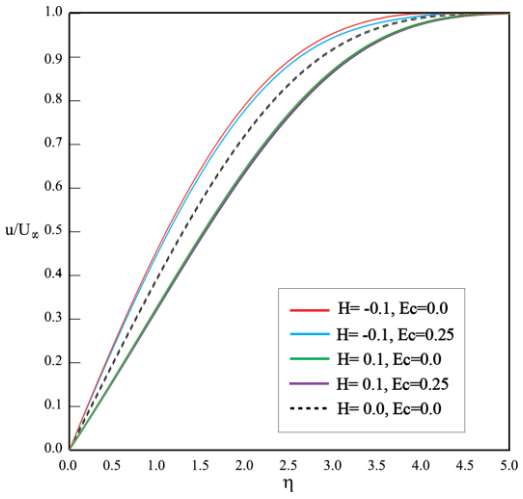

Figure 9: Velocity profile for different values of *H* and *Ec* with *Pr* = 6.2, ξ = 0.1, *Ri* = *-0.1* and ϕ = 0.04 when *Q* = *0*.

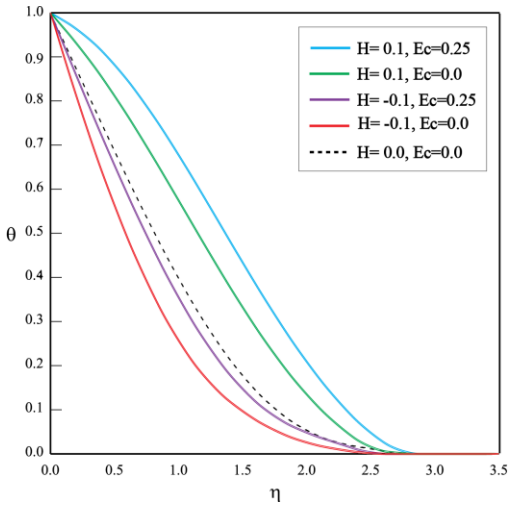

Figure 10: Temperature profile for different values of *H* and *Ec* with *Pr* = 6.2, ξ = 0.1, *Ri* = *-0.1* and ϕ = 0.04 when *Q* = *0*.

From figures 11 and 12, it is observed that increasing of viscous dissipation (*Ec*) decreases both the skin friction and heat transfer rates. Also noted that both skin

friction and heat transfer increases as the magnetic parameter ξ increases. As in the case of aiding mixed convection flow, the suction increases the local skin friction and the heat transfer rates while injection decreases them when compared to the impermeable wall case.

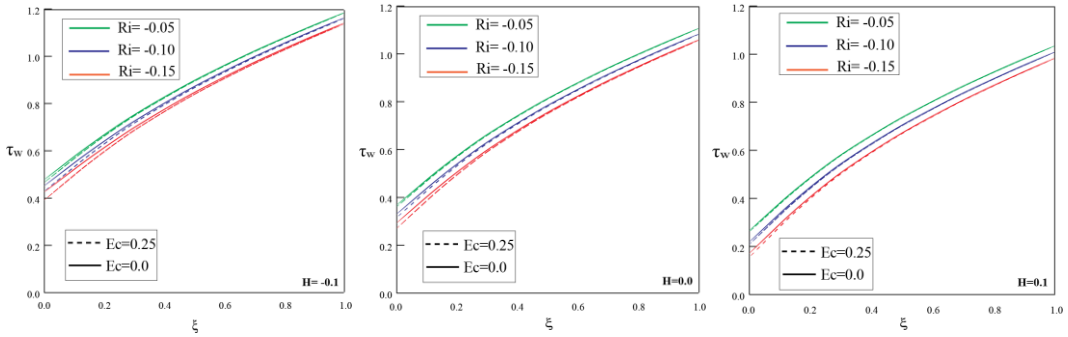

(*a*) (*b*) (*c*)

Figure 11: Effects of *Ri* (oppising-buoyancy), ξ and *Ec* on skin friction for (*a*) *H = -0.1* (suction), (*b*) *H = 0.0* and (*c*) *H = 0.1*(injection) with *Pr = 6.2* and *ϕ = 0.04* when *Q = 0.*

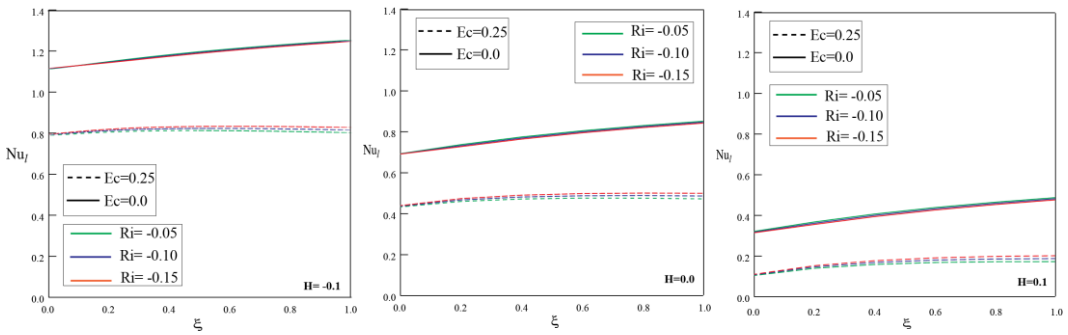

(*a*) (*b*) (*c*)

Figure 12: Effects of *Ri* (opposing-buoyancy), ξ and *Ec* on local Nusselt number for (*a*) *H = -0.1* (suction), (*b*) *H = 0.0* and (*c*) *H = 0.1*(injection) with *Pr = 6.2* and *ϕ = 0.04* when *Q = 0.*

6. Conclusion

This work deals with the effects of buoyancy parameter, transverse magnetic field, viscous dissipation and suction/injection on skin friction and surface heat transfer in Cu/H_2O nanofluid flow over a semi-infinite flat plate. The governing partial differential equations are reduced to simple polynomial equations whose coefficients are of independent parameters *Pr*, ξ, *Ri*, *H*, *Ec* and *Q*. These equations offer a practicing engineer a rapid way of obtaining shear stress and heat transfer for any combination of *Pr*, ξ, *Ri*, *H*, *Ec* and *Q*. The great advantage involved in the present technique is that the results are obtained with high order of accuracy and the amount

of calculation is certainly less when compared with more conventional methods. Hence the practicing engineers and scientists can employ this unique approximate technique as a powerful tool for solving boundary layer flow and heat transfer problems.

References

[1] Choi, U.S., 1995, "Enhancing thermal conductivity of fluids with nanoparticles" Developments and Applications of Non-Newtonian Flows, D.A.Siginer and H.P.Wang, eds., ASME. FED.231/MD., 66, pp.99-105.

[2] Masuda, H., Ebata, A., Teramae, K., and Hishinuma, N., 1993, "Alteration of thermal conductivity and viscosity of liquid by dispersing ultra-fine particles (Dispersion of γ–Al_2O_3, SiO_2 and TiO_2 ultra-fine particles)," Netsu Bussei., 7, pp.227-233.

[3] Yimin Xuan, and Qiang Li, 2003, "Investigation on Convective Heat Transfer and Flow Features of Nanofluids," Journal of Heat Transfer, 125, pp.151-155.

[4] Buongiorno, J., 2006, "Convective transport in Nanofluids," ASME J. Heat Transfer, 128, pp.240-250.

[5] Antony Raj, S., 1989, "Analytic solution for combined forced and free convection from a non-isothermal wedge," Acta Phys. Hungarica, 65, pp.59-68.

[6] Watanabe, T., 1991, "Forced and free mixed convection boundary layer flow with uniform suction or injection on a vertical flat plate," Acta Mech., 89, pp.123-132.

[7] Orhan Aydin, and Ahmet Kaya, 2009, "MHD mixed convection of a viscous dissipating fluid about a permeable vertical flat plate," Applied Mathematical Modelling, 33, pp.4086-4096.

[8] Rana, P., and Bhargava, R., 2011, "Numerical study of heat transfer enhancement in mixed convection flow along a vertical plate with heat source/sink utilizing nanofluids," Commun. Nonlinear Sci. Numer. Simulat., 16, pp.4318-4334.

[9] Chandrasekar, M., 1998, "Thermodynamical modelling of boundary layer flow with suction and injection," ASME J. Appl. Mech., 65, pp.764-768.

[10] Chandrasekar, M., 2003, "Analytical study of heat transfer and boundary layer flow with suction and injection," Heat and Mass Transfer, 40, pp.157-165.

[11] Chandrasekar, M., and Baskaran, S., 2006, "Modelling and analytical solution to heat transfer and boundary layer flow with suction and injection," J. Non-Equilibrium Thermodynamics, 31, pp.153-171.

[12] Chandrasekar, M., and Kasiviswanathan, M.S., 2015, "Magneto hydrodynamic flow with viscous dissipation effects in the presence of suction and injection," J. Theor. Appl. Mech., 53, pp.93-107.

[13] Gyarmati, I., 1969, "On the governing principle of dissipative processes and its extension to non-linear problems," Ann. Phys., 23, pp.353-378.

[14] Gyarmati, I., 1970, "Non equilibrium thermodynamics: Field theory and variational principles," Springer-Verlag, Berlin.
[15] Onsager, L., 1931, "Reciprocal relations in irreversible processes-I," Phys. Rev., 37, pp.405-406.
[16] Onsager, L., 1931, "Reciprocal relations in irreversible processes-II," Phys. Rev., 38, pp.2265-2266.
[17] Vincze, Gy., 1971, "Deduction of the quasi-linear transport equations of hydro-thermodynamics from the Gyarmati's principle," Ann. Phys., 27, pp.225-236.
[18] Lin, H.T., and Lin, L.K., 1987, "Similarity solutions for laminar forced convection heat transfer from wedges to fluids of any Prandtl number," Int. J. Heat Mass Transfer, 30, pp.1111-1118.
[19] Yih, K.A., 1999, "MHD forced convection flow adjacent to a non-isothermal wedge," Int. Comm. Heat Mass Transfer, 26, pp.819-827.
[20] Watanabe, T., and Pop, I., 1994, "Thermal boundary layers in magneto hydrodynamic flow over a flat plate in the presence of a transverse magnetic field," Acta Mech., 105, pp.233-238.
[21] Saeid, N.W., 2005, "Mixed convection flow along a vertical plate subjected to time-periodic surface temperature oscillations," Int. J. Therm. Sci., 44, pp.531-539.